Structural and Multidisciplinary Optimization manuscript No.
(will be inserted by the editor)

Efficient topology optimization with linearized buckling using reduced order modelling

NM · NM · NM · NM

Received: date / Accepted: date

Abstract **Keywords** Topology optimization, Buckling, Reduced order modelling, Combined approximations

1 Introduction

Topology optimization (TO) is a useful tool for designing structural components and materials. The simplest and frequently considered optimization problem is compliance minimization under a volume constraint. This formulation favors designs consisting of slender members in compression and tension. Unfortunately, in practical applications these structures are inherently prone to buckle, since stiffness and stability are two competing concepts. The most common way of accommodating for stability in optimization is to perform a linearized buckling analysis, and to constrain the critical buckling load factor (Neves et al. [17], Dalklint et al. [6], Gao and Ma [10], Ferrari and Sigmund [8]).

Typically, the optimization problem is solved iteratively using a nested approach whereby equilibrium equations, which constitute the majority of the computational cost, are enforced implicitly and must be solved in each iteration. Typically, several hundred design iterations need to be performed to find a local minima. This computational cost is further increased when buckling is considered, since the buckling load factors are computed from a generalized eigenvalue problem. Eigenvalue problems are notoriously difficult to solve and scale poorly with the problem size, in comparison to linear systems of equations which in the best case scale linearly with the number of unknowns. This cost becomes prohibitive for large to medium scale problems, which makes the technique unappealing for industrial applications. This motivates searching for efficient numerical methods which can alleviate this computational burden.

Recently, efforts have been made to extend TO with buckling constraints to large scale problems. Dunning et al. [7], presented a Block-Jacobi CG solver with a shift-and invert strategy based on information from previous design iterations. While this method was shown to be efficient it still requires a matrix factorization at each design update. Ferrari and Sigmund [9], instead reused the multigrid preconditioner from the initial equilibrium problem to solve the eigenvalue problem on a coarser finite element mesh. The coarse grid eigenmodes were then projected onto a finer mesh and refined using inverse iteration. This reduced the cost for solving the eigenvalue problems while retaining a good approximation of the eigenmodes. Also worth noting is the work by Bian and Fang [3], where an assembly-free eigenvalue solver was used to solve the eigenvalue problem on a grid of several million elements.

A number of methods based on reduced order modeling (ROM) have been proposed to accelerate topology optimization. In ROM the equilibrium equations are projected onto a reduced

Address(es) of author(s) should be given

solution space which is much smaller than the high-fidelity problem. The efficacy of a ROM is ultimately decided by the cost of generating the reduced space. One approach is to base the reduced space on previous solutions to the equilibrium equations, and update the space when new solution vectors become available [11, 5]. Kang et al. [13] solved the eigenvalue problem concurrently with the optimization problem, improving the accuracy sequentially.

An attractive ROM-technique for optimization problems is reanalysis, in which the system matrix's factorization in a design iteration is used to build a reduced space for subsequent iterations. The use of reanalysis to solve linear systems was first discussed by Kirsch [14]. More recently, reanalysis has been applied to topology optimization. Kirsch showed [15] that a ROM using reanalysis is equivalent to a preconditioned conjugate gradient method for linear systems of equations. Amir et al. [1] studied reanalysis for compliance problems and discussed the idea of a consistent sensitivity analysis, i.e. where the inaccuracies in the ROM are taken into account. Senne et al. [18] extended reanalysis to problems with geometric and material nonlinearities. Bogomolny [4] ~~extended~~ used reanalysis ~~to~~ for vibrational problems, wherein a reduced order model was built for each sought eigenpair. For the generalized eigenvalue problem the basis vectors must be orthogonalized to ensure that the correct eigenpair is approximated. ~~Bogomolny also derives a consistent sensitivity analysis for the vibrational problem~~.

In this paper, we aim to show that ROM using Combined Approximation can effectively be implemented for buckling problems. What makes this work unique is that CA will be used for the linear analysis, generalized eigenproblem and the adjoints.

2 Preliminaries

sec:prelim

We consider the finite element discretized linear system

$$\mathbf{K}_L \mathbf{u}_o = \mathbf{F}_o, \tag{1}$$

mech

in combination with appropriate boundary conditions to describe our mechanical system. In (1), $\mathbf{K}_L \in \mathbb{R}^{n\times n}$ is the symmetric and positive definite linear stiffness matrix , $\mathbf{u}_o \in \mathbb{R}^n$ is the reference displacement vector and $\mathbf{F}_o \in \mathbb{R}^n$ the load vector, where n is the number of degrees-of-freedom. To solve (1), we utilize the Cholesky decomposition of $\mathbf{K}_L$ in combination with forward/backward substitutions, i.e.

$$\mathbf{K}_L = \mathbf{U}^T\mathbf{U}, \tag{2}$$

mechFac01

where $\mathbf{U} \in \mathbb{R}^{n\times n}$ is upper triangular. After solving (1) for $\mathbf{u}_o$ using (2), we compute the symmetric and indefinite stress stiffness matrix $\mathbf{K}_G(\mathbf{u}_o) \in \mathbb{R}^{n\times n}$, which enables the generalized eigenvalue problem

$$(\mathbf{K}_L + \lambda_j \mathbf{K}_G(\mathbf{u}_o))\,\boldsymbol{\phi}_j = \mathbf{0}, \quad j \in \mathbb{N}_n, \tag{3}$$

lineig01

to be solved for the eigenpairs $(\lambda_j, \boldsymbol{\phi}_j) \in (\mathbb{R}\times\mathbb{R}^n)$. However, since $\mathbf{K}_G$ is indefinite, it is convenient to pose (3) as

$$(\mathbf{K}_G(\mathbf{u}_o) - \mu_j \mathbf{K}_L)\,\boldsymbol{\phi}_j = \mathbf{0}, \quad j \in \mathbb{N}_n, \tag{4}$$

lineig02

where $\mu_j = -\frac{1}{\lambda_j}$ and we assume that $\boldsymbol{\phi}_i^T \mathbf{K}_L \boldsymbol{\phi}_j = \delta_{ij}$. Solving the generalized eigenvalue problem in (3) or (4), is referred to as *linearized buckling analysis*, wherefore the eigenvalues λ_j are denoted the critical load factors, so that the critical load is $\mathbf{F}_i = \lambda_i \mathbf{F}_o$. The eigenmode associated with the critical load $\mathbf{F}_i$ is $\boldsymbol{\phi}_i$.

3 Reduced order modelling

sec:CA

The basic idea of reduced order modelling (ROM) is to approximate solutions to linear systems using a reduced basis, i.e

$$\mathbf{u}_0 \approx \tilde{\mathbf{u}}_0 = \alpha_1\mathbf{u}_1 + \alpha_2\mathbf{u}_2 + \ldots\alpha_m\mathbf{u}_m \tag{5}$$

eq:rom1

where $\mathbf{u}_i$ are the basis vectors and α_i the reduced model coefficients. The number of bases, m, is significantly smaller that the dimension of the full problem, i.e. $m \ll n$. The reduced model coefficients are usually found by inserting the approximation into the equilibrium equation, which is finally projected onto the basis $\mathbf{u}_i$ by premultiplying with $\mathbf{R} = [\mathbf{u}_1, ...\mathbf{u}_m]$. This is also known as projection based reduced order modelling. The success of the ROM method relies on the choice of the basis vectors, $\mathbf{u}_i$. In this work the basis vectors will be generated by Combined Approximation (CA). The idea is to reuse the factorization of the stiffness matrix corresponding to a previous design iteration.

3.1 Reanalysis of the linear equilibrium problem

Let us start by considering the approximate solution of (1). Let ρ_j be the design variables at optimization iteration j. In the CA approach, we utilize the factorization of $\mathbf{K}_L(\rho_{k-n}) = \overline{\mathbf{K}}_L$ from a previous design iteration, to compute the displacement in the current design iteration, i.e.

$$\left(\overline{\mathbf{K}}_L + \Delta\mathbf{K}_L\right)\mathbf{u}_0 = \mathbf{F}_0, \tag{6}$$ mech02

where $\Delta\mathbf{K}_L$ is the change in stiffness due to the design change. Multiplying (6) by $\overline{\mathbf{K}}_L^{-1}$ yields

$$\left(\mathbf{I} + \mathbf{K}_L^{-1}\Delta\overline{\mathbf{K}}_L\right)\mathbf{u}_0 = \overline{\mathbf{K}}_L^{-1}\mathbf{F}_0. \tag{7}$$ mech03

It can be shown that the inverse of $(\mathbf{I} + \overline{\mathbf{K}}_L^{-1}\Delta\mathbf{K}_L)$ exists as a power series if $\left\|\overline{\mathbf{K}}_L^{-1}\Delta\mathbf{K}_L\right\|_2 < 1$, hence

$$(\mathbf{I} + \mathbf{B})^{-1} = \sum_{k=0}^{\infty}(-\mathbf{B})^k, \quad \text{where} \quad \mathbf{B} = \overline{\mathbf{K}}_L^{-1}\Delta\mathbf{K}_L. \tag{8}$$ mech04

The solution to (7) can therefore be expressed as

$$\mathbf{u}_0 = \left(\mathbf{I} - \mathbf{B} + \mathbf{B}^2 - \ldots\right)\overline{\mathbf{K}}_L^{-1}\mathbf{F}_0. \tag{9}$$ mech05

The idea of CA is to truncate the infinite power series (8) at e.g. $s \ll n$, and assume that the approximative solution is spanned by this basis, i.e.

$$\tilde{\mathbf{u}}_0 = y_1\mathbf{u}_1 + y_2\mathbf{u}_2 + \ldots + y_s\mathbf{u}_s = \mathbf{R}\mathbf{y}, \tag{10}$$ uapprox

where $\mathbf{R} = [\mathbf{u}_1, \mathbf{u}_2, ...\mathbf{u}_s] \in \mathbb{R}^{n\times s}$is the matrix of basis vectors and $\mathbf{y} \in \mathbb{R}^s$ is the vector of reduced model coefficients. Finally, we orthogonalize the basis vectors with respect to $\mathbf{K}_L$, obtaining a fully decoupled system of equations. The basis vectors are obtained recursively from (9) as

$$\begin{aligned}
&\mathbf{u}_1 = \overline{\mathbf{K}}_L^{-1}\mathbf{F}_0, \\
&\mathbf{u}_i = -\mathbf{B}\mathbf{t}_{i-1}, && i = 2, ..., s, \\
&\mathbf{t}_j = \mathbf{u}_i(\mathbf{u}_i^T\mathbf{u}_i)^{-1/2}, && i = 1, ..., s, \\
&\mathbf{r}_i = \mathbf{u}_i - \sum_{j=1}^{i-1}\left(\mathbf{t}_i^T\mathbf{K}_L\mathbf{v}_j\right)\mathbf{v}_j, && i = 1, ..., s, \\
&\mathbf{v}_i = \mathbf{r}_i\left(\mathbf{r}_i^T\mathbf{K}_L\mathbf{r}_i\right)^{-1/2}, && i = 1, ..., s.
\end{aligned} \tag{11}$$ basisvec

where $\mathbf{u}_1$ is known from the previous optimization step. Now, replacing the exact solution $\mathbf{u}_0$ in (1) with the approximation $\tilde{\mathbf{u}}_0 = \mathbf{R}\mathbf{y}$ and premultiplying both sides with $\mathbf{R}^T$ yields $\mathbf{y} = \mathbf{R}^T\mathbf{F}_0$. The approximation can then be recovered from (10)

$$\tilde{\mathbf{u}}_0 = \mathbf{R}\mathbf{R}^T\mathbf{F}_0 \tag{12}$$ eq:static_soluti

3.2 Reanalysis of the buckling problem

Let us now turn to approximating the j:th eigenpair of (4). The idea is to generate a set of basis vectors for each eigenpair, and to approximate the j:th eigenmode as

$$\tilde{\boldsymbol{\phi}}_j = y_{1j}\mathbf{u}_{1j} + y_{2j}\mathbf{u}_{2j} + ...y_{sj}\mathbf{u}_{sj} = \mathbf{R}_j\mathbf{y}_j. \tag{13}$$ phiapprox

where the matrix of basis vectors is $\mathbf{R}_j = [\mathbf{u}_{1j}, \mathbf{u}_{2j}, ..., \mathbf{u}_{sj}] \in \mathbb{R}^{n\times s}$ and the reduced model eigenmode is $\mathbf{y} \in \mathbb{R}^s$. The eigenvalue corresponding to the approximation in (13) can then be approximated using Rayleigh quotients. To generate the basis vectors we again utilize the factorization of $\overline{\mathbf{K}}_L$ this time applied to (4), i.e.

$$\mathbf{K}_G\boldsymbol{\phi}_j = \mu_j\left(\overline{\mathbf{K}}_L + \Delta\mathbf{K}_L\right)\boldsymbol{\phi}_j, \quad j \in \mathbb{N}_n. \tag{14}$$ eig01

Premultiplication of (14) by $\overline{\mathbf{K}}_L^{-1}$ yields

$$\overline{\mathbf{K}}_L^{-1}\mathbf{K}_G\boldsymbol{\phi}_j = \mu_j\left(\mathbf{I} + \mathbf{B}\right)\boldsymbol{\phi}_j, \quad j \in \mathbb{N}_n. \tag{15}$$ eig02

As before, the inverse of $(\mathbf{I} + \mathbf{B})$ exists as a power series if $\|\mathbf{B}\|_2 < 1$, i.e.

$$\boldsymbol{\phi}_j = \frac{1}{\mu_j}\left(\mathbf{I} - \mathbf{B} + \mathbf{B}^2 - \ldots\right)\overline{\mathbf{K}}_L^{-1}\mathbf{K}_G\boldsymbol{\phi}_j, \quad j \in \mathbb{N}_n, \tag{16}$$ eig03

The approximation to $\boldsymbol{\phi}_j$, i.e. $\tilde{\boldsymbol{\phi}}_j$, is obtained by truncating the infinite sum at term $s \ll n$ and substituting $\boldsymbol{\phi}_j$ for $\overline{\boldsymbol{\phi}}_j$ the j:th eigenvector corresponding to the matrix $\overline{\mathbf{K}}_L$. To obtain an improved set of basis vectors, we employ deflation, i.e. Gram-Schmidt orthogonalization. In this way, the basis generation can be defined recursively as

$$\begin{aligned}
&\mathbf{u}_{1j} = \overline{\mathbf{K}}_L^{-1}\mathbf{K}_G\overline{\boldsymbol{\phi}}_j, \\
&\mathbf{u}_{ij} = -\mathbf{B}\mathbf{t}_{(i-1)j}, && i = 2, ..., s, \\
&\mathbf{t}_{ij} = \mathbf{u}_{ij}\left(\mathbf{u}_{ij}^T\mathbf{K}_L\mathbf{u}_{ij}\right)^{-1/2}, && i = 1, ..., s, \\
&\mathbf{v}_{ij} = \mathbf{t}_{ij} - \textstyle\sum_{j=1}^{k-1}\left(\tilde{\boldsymbol{\phi}}_j^T\mathbf{K}_L\mathbf{t}_{ij}\right)\tilde{\boldsymbol{\phi}}_j, && i = 1, ..., s.
\end{aligned} \tag{17}$$ phibasisvec2

Now, inserting the approximation in (13) into (4) and premultiplying by $\mathbf{R}_j$ gives the reduced system

$$\left(\mathbf{K}_G^R(\mathbf{u}_0) - \tilde{\mu}_j\mathbf{K}_L^R\right)\mathbf{y}_j = 0, \tag{18}$$ eq:redeig

where $\mathbf{K}_G^R(\mathbf{u}_0) = \mathbf{R}_j^T\mathbf{K}_G(\mathbf{u}_0)\mathbf{R}_j$ and $\mathbf{K}_L^R = \mathbf{R}_j^T\mathbf{K}_L\mathbf{R}_j$. Thus, for each sought eigenpair, the procedure is to first generate one set of basis vectors according to (17), and to then solve (18) for the largest magnitude eigenpair. We will then let $(\tilde{\mu}_j, \mathbf{R}_j\mathbf{y}_j)$ be an approximation to the j:th eigenpair.

4 Design representation, filtration and thresholding

The goal of our topology optimization is to optimally distribute a linear elastic material in the design domain, $\Omega \in \mathbb{R}^3$, which is quantified by the continuous non-dimensional volume fraction field $z : \Omega \to [0, 1]$. A well-posed optimization problem is obtained using restriction, by which fine-scale oscillations of z are penalized via the Helmholtz PDE-filter, cf. [16]. In this way, z is replaced by the smooth field $\nu : \Omega \to [0, 1]$, which can be expressed as

$$\mathbf{K}_\nu\boldsymbol{\nu} = \mathbf{F}_\nu\mathbf{z}. \tag{19}$$ eq:filter

To limit regions wherein $\nu(\boldsymbol{X}) \in (0,1)$, we use thresholding [12, 21] and penalization [2], such that

$$\begin{aligned} &\mathbf{D} = \chi_L(\bar{\nu})\mathbf{D}_o \quad \text{and} \quad \mathbf{G} = \chi_G(\bar{\nu})\mathbf{G}_o, \\ &\text{where} \quad \chi_L(\bar{\nu}) = \delta_o + \bar{\nu}^q(1-\delta_o), \quad \chi_G(\bar{\nu}) = \bar{\nu}^q, \\ &\text{and} \quad \bar{\nu} = H_{\beta,\eta}(\nu) = \frac{\tanh(\beta\eta) + \tanh(\beta(\nu-\eta))}{\tanh(\beta\eta) + \tanh(\beta(1-\eta))}. \end{aligned} \tag{20}$$

matInter

In (20), β and η are scalars defined such that $\lim_{\beta\to\infty} H_{\beta,\eta}(\nu) = u_s(\nu-\eta)$, where u_s is the unit step function. Increasing values of $q \in \mathbb{R}^+$ enforce increasing levels of penalization, and $\delta_o \in \mathbb{R}^+$ is the ersatz material stiffness scaling. Henceforth, we consider

$$\begin{aligned} \mathbf{K}_L(\rho) &= \sum\sum \int_\Omega \chi_L(\rho)\mathbf{B}^T\mathbf{D}\mathbf{B}\, dV \\ \mathbf{K}_G(\rho, \mathbf{u}(\rho)) &= \sum\sum \int_\Omega \chi_G(\rho)\mathbf{Y}^T\mathbf{G}(\mathbf{u})\mathbf{Y}\, dV, \end{aligned} \tag{21}$$

Kg

where $\mathbf{B}$ and $\mathbf{G}$ contains the gradient of the element shape functions, $\mathbf{Y}$ is a symmetric block matrix of the stresses and $\mathbf{D}$ is the Voigt representation of the material tangent.

4.1 Aggregation

In this work a lower bound is set on the lowest buckling load factor. However, it is well known that the min-function is not differentiable. For this reason the critical buckling load factor is approximated using the p-norm (see Torii and De Faria [20]), which aggregates the n_{eval} lowest buckling load factors. In practice, we instead put an upper bound on the reciprocal value $\gamma = \lambda^{-1}$. The constraint on the critical buckling load factor is stated as

$$\gamma_c = \max \gamma_k \approx \left(\sum_{i=1}^{n_{\text{eval}}} \gamma_i^p \right)^{1/p} \leq \gamma^*. \tag{22}$$

eq:pnorm

where γ^* is the upper bound on γ_c. As $p \to \infty$ we retrieve γ_c. Aggregating the buckling load factor avoids issues when two BLF's coincide wherein the min-function is not differentiable, as opposed to the p-norm.

5 Optimization formulation

We use the topology optimization to solve the problem presented below

$$(\mathbb{TO}) \begin{cases} \min\limits_{\mathbf{z}} \;\; g_o = \mathbf{F}^T\mathbf{u}, \\ \text{s.t} \quad \begin{cases} g_1 = \int_\Omega \bar{\nu}\, dV - V_{max} \leq 0, \\ g_2 = \gamma \leq \gamma^\star, \\ 0 \leq \mathsf{z}_e \leq 1, \quad e = 1, ..., N_e, \end{cases} \end{cases} \tag{23}$$

TO

which is a standard compliance minimization problem subject to an lower bound constraint on the critical buckling load factor and a maximum volume constraint.

5.1 Sensitivity analysis

When computing the sensitivity of a non self-adjoint displacement dependent function, the implicit sensitivity of the displacements with respect to the design variables appears. In this work, we annihilate this implicit sensitivity through the adjoint method. To exemplify this process, we introduce the augmented version of a general function $g = g(\boldsymbol{\nu}(\mathbf{z}), \mathbf{u}(\boldsymbol{\nu}(\mathbf{z})))$ as

$$g := g - \boldsymbol{\Lambda}^T \mathbf{r} - \boldsymbol{\Lambda}_{\boldsymbol{\nu}}^T \mathbf{r}_{\boldsymbol{\nu}}, \tag{24}$$ gensens01

where $\mathbf{r} = \mathbf{K}_L \mathbf{u} - \mathbf{F}$ and $\mathbf{r}_{\boldsymbol{\nu}} = \mathbf{K}_{\boldsymbol{\nu}} \boldsymbol{\nu} - \mathbf{F}_{\boldsymbol{\nu}} \mathbf{z}$. The sensitivity of (24) with respect to $\mathbf{z}$ is

$$\frac{dg}{d\mathbf{z}} = \frac{\partial g}{\partial \boldsymbol{\nu}} \frac{\partial \boldsymbol{\nu}}{\partial \mathbf{z}} + \frac{\partial g}{\partial \mathbf{u}} \frac{\partial \mathbf{u}}{\partial \boldsymbol{\nu}} \frac{\partial \boldsymbol{\nu}}{\partial \mathbf{z}} - \boldsymbol{\Lambda}^T \left(\frac{\partial \mathbf{r}}{\partial \boldsymbol{\nu}} \frac{\partial \boldsymbol{\nu}}{\partial \mathbf{z}} + \frac{\partial \mathbf{r}}{\partial \mathbf{u}} \frac{\partial \mathbf{u}}{\partial \boldsymbol{\nu}} \frac{\partial \boldsymbol{\nu}}{\partial \mathbf{z}} \right) - \boldsymbol{\Lambda}_{\boldsymbol{\nu}}^T \left(\frac{\partial \mathbf{r}_{\boldsymbol{\nu}}}{\partial \mathbf{z}} + \frac{\partial \mathbf{r}_{\boldsymbol{\nu}}}{\partial \boldsymbol{\nu}} \frac{\partial \boldsymbol{\nu}}{\partial \mathbf{z}} \right), \tag{25}$$ gensens02

which can be rearranged to

$$\frac{dg}{d\mathbf{z}} = -\boldsymbol{\Lambda}_{\boldsymbol{\nu}}^T \frac{\partial \mathbf{r}_{\boldsymbol{\nu}}}{\partial \mathbf{z}} + \left[\frac{\partial g}{\partial \boldsymbol{\nu}} - \boldsymbol{\Lambda}^T \frac{\partial \mathbf{r}}{\partial \boldsymbol{\nu}} - \boldsymbol{\Lambda}_{\boldsymbol{\nu}}^T \frac{\partial \mathbf{r}_{\boldsymbol{\nu}}}{\partial \boldsymbol{\nu}} + \left(\frac{\partial g}{\partial \mathbf{u}} - \boldsymbol{\Lambda}^T \frac{\partial \mathbf{r}}{\partial \mathbf{u}} \right) \frac{\partial \mathbf{u}}{\partial \boldsymbol{\nu}} \right] \frac{\partial \boldsymbol{\nu}}{\partial \mathbf{z}}. \tag{26}$$ gensens03

Here, we find that the implicit $\frac{\partial \mathbf{u}}{\partial \boldsymbol{\nu}}$ and $\frac{\partial \boldsymbol{\nu}}{\partial \mathbf{z}}$ sensitivities are annihilated by sequentially solving the coupled linear systems

$$\begin{aligned} \mathbf{K}_L \boldsymbol{\Lambda} &= \frac{\partial g}{\partial \mathbf{u}}, \\ \mathbf{K}_{\boldsymbol{\nu}} \boldsymbol{\Lambda}_{\boldsymbol{\nu}} &= \frac{\partial g}{\partial \boldsymbol{\nu}} - \boldsymbol{\Lambda}^T \mathbf{K}_{\boldsymbol{\nu}}, \end{aligned} \tag{27}$$ gensen04

which yields the final expression for the sensitivity of g as

$$\frac{dg}{d\mathbf{z}} = -\boldsymbol{\Lambda}_{\boldsymbol{\nu}}^T \frac{\partial \mathbf{r}_{\boldsymbol{\nu}}}{\partial \mathbf{z}} \tag{28}$$ gensens05

When seeking the sensitivity of the buckling load factor μ_j for $j \in \mathbb{N}_n$, we let $g = \mu_j$ and compute $\frac{\partial g}{\partial \mathbf{u}}$ and $\frac{\partial g}{\partial \boldsymbol{\nu}}$ from the differentiations of (4), i.e.

$$\begin{aligned} \frac{\partial \mu_j}{\partial \mathbf{u}} &= \boldsymbol{\phi}_j^T \frac{\partial \mathbf{K}_G}{\partial \boldsymbol{\nu}} \boldsymbol{\phi}_j, \\ \frac{\partial \mu_j}{\partial \boldsymbol{\nu}} &= \boldsymbol{\phi}_j^T \left(\frac{\partial \mathbf{K}_G}{\partial \boldsymbol{\nu}} - \mu_j \frac{\partial \mathbf{K}_L}{\partial \boldsymbol{\nu}} \right) \boldsymbol{\phi}_j. \end{aligned} \tag{29}$$ bucklingsens01

Meaning, to compute the sensitivity of each buckling load factor we must solve a linear equation according to (27).

5.2 Consistent sensitivity analysis

The sensitivities in the previous section assume that the initial equilibrium (1) and buckling problem (3) are solved exactly. However, in this work they are solved approximately, meaning there is a residual $\mathbf{r}_{\mathbf{u}_0} = \mathbf{F}_0 - \mathbf{K}_L \tilde{\mathbf{u}}_0$ and residuals $\mathbf{r}_{\boldsymbol{\Phi}_j} = (\mathbf{K}_G - \mu_j \mathbf{K}_L) \tilde{\boldsymbol{\phi}}_j$. These inaccuracies can be accounted for (see Amir et al. [1] and Bogomolny [4]) at the cost of introducing more adjoint vectors which require backward and forward substitution of the factorized stiffness matrix. Although accounting for the inaccuracies this way might be mathematically satisfying the consistent sensitivities ultimately reflect the approximate problem, not the exact problem. Meaning they are accurate with regard to the inaccurate problem, which is not the problem we wish to solve. We hope to show that if the equilibrium equations are solved accurately enough then using the sensitivities of the exact problem will lead to the correct design. Furthermore, the adjoint equations in (27) are also solved using a CA-approach.

For a consistent sensitivity analysis of the buckling load factors we refer to the appendix.

6 Numerical examples

sec:examples

We demonstrate the reduced order model on three different geometries, see figures 1, 3 and 5. The optimization problem (23) is solved using Svanbergs MMA solver, with default parameters see [19] for details. Young's modulus and Poisson's ratio are set to 2×10^5 and $\nu = 0.3$. Continuation is used for the material penalization in (20), where $q = 2$ initially and is incremented by 0.5 every 20 iterations until $q = 6$, and the ersatz material stiffness scaling is set to $\delta_0 = 1 \times 10^{-6}$. The penalty exponent of the p-norm is set to $p = 8$ initially and is amplified to 64 once the material penalization reaches $q = 6$. Finally, the filtered densities are penalized using a smooth Heaviside approximation according to (20), where $\beta = 6$ and $\eta = 0.5$.

The problems are solved without the reduced order models described in section 3, that is using direct solvers, to get a reference solution.

6.1 Axially loaded rod

The geometry is described by figure 1 with $L_x = 400$ and $L_y = 80$. The filter radius is set to 4 and the allowed volume fraction is set to 0.50.

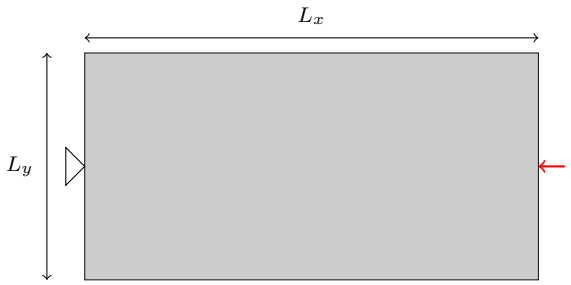

Fig. 1 Geometry of column

fig:geometry_colu

Fig. 2 Solution using exact analysis. Yellow regions indicate presence of material, blue regions absence.

fig:column_ref

6.2 Spire structure

The geometry is described by figure 3 with $L_x = 240$ and $L_y = 120$. The filter radius is set to 6 and the allowed volume fraction is set to 0.35.

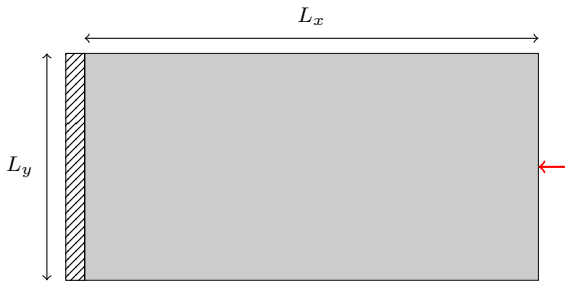

Fig. 3 Geometry of spire

fig:geometry_spi

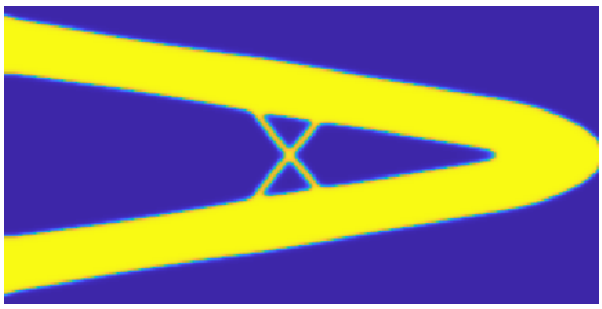

Fig. 4 Solution using exact analysis. Yellow regions indicate presence of material, blue regions absence.

fig:spire_ref

6.3 V structure

The geometry is described by figure 5 with $L_x = 280$ and $L_y = 120$. The filter radius is set to 6 and the allowed volume fraction is set to 0.18.

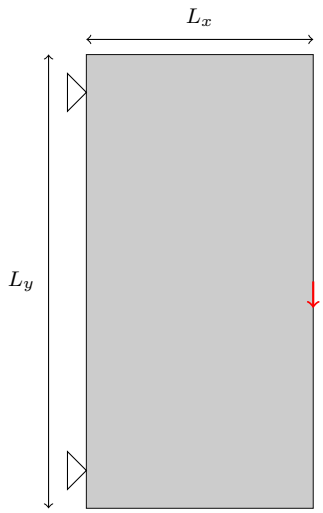

Fig. 5 Geometry of twobar

fig:geometry_two

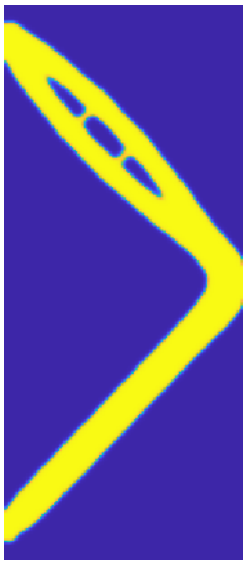

Fig. 6 Solution using exact analysis. Yellow regions indicate presence of material, blue regions absence. fig:twobar_ref

7 Conclusions

sec:conclusions

Acknowledgements

We would like to thank Krister Svanberg for his implementation of MMA in MATLAB.

Replication of results

All MATLAB code is provided as supplementary material.

Conflict of interest

On behalf of all authors, the corresponding author states that there is no conflict of interest.

References

mir2009approximate
1. Amir, O., Bendsøe, M.P., Sigmund, O., 2009. Approximate reanalysis in topology optimization. International Journal for Numerical Methods in Engineering 78, 1474–1491.

bendsoe1989optimal
2. Bendsøe, M.P., 1989. Optimal shape design as a material distribution problem. Structural optimization 1, 193–202.

bian2017large
3. Bian, X., Fang, Z., 2017. Large-scale buckling-constrained topology optimization based on assembly-free finite element analysis. Advances in Mechanical Engineering 9, 1687814017715422. doi:10.1177/1687814017715422.

omolny2010topology
4. Bogomolny, M., 2010. Topology optimization for free vibrations using combined approximations. International Journal for Numerical Methods in Engineering 82, 617–636.

oi2019accelerating
5. Choi, Y., Oxberry, G., White, D., Kirchdoerfer, T., 2019. Accelerating design optimization using reduced order models. arXiv preprint arXiv:1909.11320 .

lint2021structural
6. Dalklint, A., Wallin, M., Tortorelli, D.A., 2021. Structural stability and artificial buckling modes in topology optimization. Structural and Multidisciplinary Optimization 64, 1751–1763.

dunning2016level 7. Dunning, P.D., Ovtchinnikov, E., Scott, J., Kim, H.A., 2016. Level-set topology optimization with many linear buckling constraints using an efficient and robust eigensolver. International Journal for Numerical Methods in Engineering 107, 1029–1053.

rari2019revisiting 8. Ferrari, F., Sigmund, O., 2019. Revisiting topology optimization with buckling constraints. Structural and Multidisciplinary Optimization 59, 1401–1415.

ferrari2020towards 9. Ferrari, F., Sigmund, O., 2020. Towards solving large-scale topology optimization problems with buckling constraints at the cost of linear analyses. Computer Methods in Applied Mechanics and Engineering 363, 112911.

gao2015topology 10. Gao, X., Ma, H., 2015. Topology optimization of continuum structures under buckling constraints. Computers & Structures 157, 142–152.

gogu2015improving 11. Gogu, C., 2015. Improving the efficiency of large scale topology optimization through on-the-fly reduced order model construction. International Journal for Numerical Methods in Engineering 101, 281–304.

guest2004achieving 12. Guest, J.K., Prévost, J.H., Belytschko, T., 2004. Achieving minimum length scale in topology optimization using nodal design variables and projection functions. International journal for numerical methods in engineering 61, 238–254.

kang2020method 13. Kang, Z., He, J., Shi, L., Miao, Z., 2020. A method using successive iteration of analysis and design for large-scale topology optimization considering eigenfrequencies. Computer Methods in Applied Mechanics and Engineering 362, 112847.

rsch2008reanalysis 14. Kirsch, U., 2008. Reanalysis of structures. Springer.

kirsch2002accurate 15. Kirsch, U., Kocvara, M., Zowe, J., 2002. Accurate reanalysis of structures by a preconditioned conjugate gradient method. International Journal for Numerical Methods in Engineering 55, 233–251.

lazarov2011filters 16. Lazarov, B.S., Sigmund, O., 2011. Filters in topology optimization based on helmholtz-type differential equations. International Journal for Numerical Methods in Engineering 86, 765–781.

ves1995generalized 17. Neves, M., Rodrigues, H., Guedes, J., 1995. Generalized topology design of structures with a buckling load criterion. Structural optimization 10, 71–78.

senne2022inexact 18. Senne, T.A., Gomes, F.A., Santos, S.A., 2022. Inexact newton method with iterative combined approximations in the topology optimization of geometrically nonlinear elastic structures and compliant mechanisms. Optimization and Engineering , 1–36.

svanberg1987method 19. Svanberg, K., 1987. The method of moving asymptotes—a new method for structural optimization. International journal for numerical methods in engineering 24, 359–373.

orii2017structural 20. Torii, A.J., De Faria, J.R., 2017. Structural optimization considering smallest magnitude eigenvalues: a smooth approximation. Journal of the Brazilian Society of Mechanical Sciences and Engineering 39, 1745–1754.

g2014interpolation 21. Wang, F., Lazarov, B.S., Sigmund, O., Jensen, J.S., 2014. Interpolation scheme for fictitious domain techniques and topology optimization of finite strain elastic problems. Computer Methods in Applied Mechanics and Engineering 276, 453–472.